

Coulomb and Spin blockade of two few-electrons quantum dots in series in the co-tunneling regime

M. Ciorga,^{1,*} M. Pioro-Ladrière,^{1,2} P. Zawadzki,¹ J. Lapointe,¹ Z. Wasilewski,¹ and A. S. Sachrajda¹

¹*Institute for Microstructural Sciences, National Research Council of Canada, Ottawa, Canada K1A0R6*

²*Centre de Recherche sur les Propriétés Électroniques de Matériaux Avancés,
Université de Sherbrooke, Sherbrooke, Québec, J1K 2R1 Canada*

We present Coulomb Blockade measurements of two few-electron quantum dots in series which are configured such that the electrochemical potential of one of the two dots is aligned with spin-selective leads. The charge transfer through the system requires co-tunneling through the second dot which is *not* in resonance with the leads. The observed amplitude modulation of the resulting current is found to reflect spin blockade events occurring through either of the two dots. We also confirm that charge redistribution events occurring in the off-resonance dot are detected indirectly via changes in the electrochemical potential of the aligned dot.

PACS numbers: 73.21.La (Quantum dots), 73.23.Hk (Coulomb blockade, single-electron tunnelling), 85.75.Hh (Spin polarized field effect transistors)

I. INTRODUCTION

Semiconductor quantum dots (QDs), often referred to as “artificial atoms”,¹ have been studied intensively over the last decade. The spin of an electron confined within a QD has even been suggested as a possible physical realization of a quantum bit.² Recent progress in QD related research includes the experimental realization and study of few-electron single^{3,4} and double^{5,6} electrostatic quantum dots and the implementation of non-local charge detectors to indirectly detect a change in the number of confined electrons.^{5,7}

The most common experimental transport technique used to investigate properties of quantum dots is Coulomb blockade (CB) spectroscopy,⁸ from which the addition spectrum of the system can easily be obtained. CB techniques take advantage of the fact that to add an $N + 1$ electron to a N -electron dot (i.e. to observe a CB peak) one needs to match the electro-chemical potential of the quantum dot to that of the leads. The electro-chemical potential of the dot, $\mu(N + 1)$, can be tuned by means of a “plunger” electrode. Since $\mu(N + 1) = E(N + 1) - E(N)$, where $E(N)$ is the ground state (GS) energy of the N -electron dot, any transition in the GS of either the N or $N + 1$ electron dots is reflected in $\mu(N + 1)$ and therefore in the plunger electrode position of the CB peak. When the dot is connected to spin selective leads the tunneling rates for each spin species are different resulting in a spin blockade mechanism.⁹ Spin blockade effects provide direct information about spin transitions through an analysis of the peak amplitude. In particular this technique can resolve whether the spin of two neighboring ground states differ by $+$ or $-1/2$. However, it is important to note that this technique relies on simultaneously measuring the property of dots with two consecutive electron numbers, N and $N + 1$. For important but relatively straightforward spin phenomena such as the ‘singlet-triplet’ transition for two or more electrons this will not be a limitation. However, for more com-

plex states such as those involving correlations, e.g spin textures,⁴ it is no longer clear that states with successive occupation numbers will overlap. In this case Coulomb blockade measurements would automatically lead to a suppressed peak amplitude thereby requiring a different procedure to study these novel phenomena. Any technique which probes electron transitions at a fixed electron number, such as the one described in this paper, may therefore be beneficial in the future for studying these more complex spin phenomena experimentally.

For quantum dot devices a condition of fixed N is met in the Coulomb blockaded regions when a dot is off resonance with the leads and, as a result, the current is strongly suppressed. At low temperatures, however, a small current still can be observed due to higher order tunneling events. Since these involve simultaneous tunneling of two or more electrons they are referred to as *co-tunneling*¹⁰ events. For very low temperatures and low bias voltages, including the experiments described in this paper, co-tunneling is dominated by elastic channels which do not involve excited electron-hole pairs within the dot. Initially treated as a limitation on the accuracy of single electron devices, electron co-tunneling processes have recently been used to probe large¹¹ and small¹² Coulomb blockaded quantum dots as well as Kondo systems.¹³

In this paper we present Coulomb and spin blockade measurements of a double quantum dot device connected to spin selective leads. In previous experiments we used a spin polarized current to probe a two-level molecule formed in the regime of filling factor $\nu = 2$ within the dots, in which the two dots were simultaneously brought into resonance with the leads.⁶ Here, by contrast, we focus on the situation when one of the dots is purposely kept off-resonance. The measured current then requires a co-tunneling process through the off-resonance dot. In order to study the consequences of ground state transitions on the co-tunneling current we sweep the perpendicular magnetic field close to the well understood $\nu = 2$ transition. A strong amplitude modulation of CB peaks

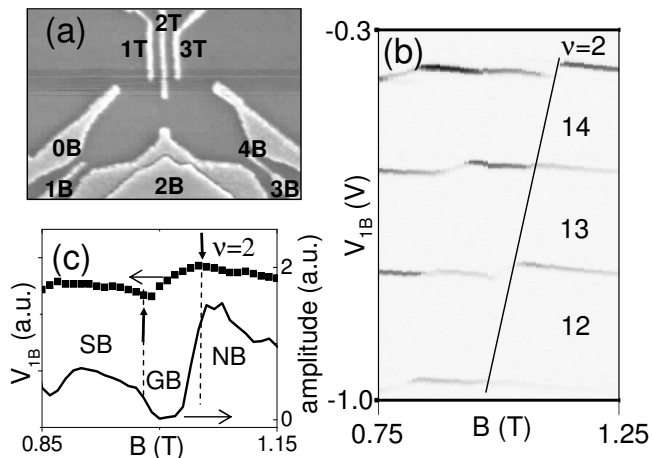


FIG. 1: (a) SEM picture of the experimental device; (b) inverted greyscale of conductance through the left dot for four CB peaks in the vicinity of $\nu = 2$. Dark (light) regions represent high (low) amplitude of CB peak; (c) typical modulation of position and amplitude of a CB peak at $\nu = 2$ transition, shown in case of the $12 \leftrightarrow 13$ transition.

is observed in the co-tunneling current. The observed modulation pattern is explained in terms of geometrical and spin blockade effects occurring in either or both dots. The results for the two dots in series are compared directly to measurements from the individual dots. It is shown that this amplitude modulation comparison can be used to identify the dominant active co-tunneling process. In addition we observe that charge redistributions associated with magnetic field induced ground state transitions in the off-resonance dot, which enjoys a fixed electron number, are reflected in changes of the electrochemical potential of the on-resonance dot.

II. EXPERIMENTAL RESULTS

A scanning electron microscope (SEM) picture of the experimental device is shown in Fig. 1(a). The device is composed of eight metallic gates deposited on the surface of a GaAs-AlGaAs heterostructure with a two-dimensional electron gas (2DEG) 90 nm below the surface. The density and mobility of 2DEG were $n = 1.7 \times 10^{11} \text{ cm}^{-2}$ and $\mu = 2 \times 10^6 \text{ cm}^2 \text{ V}^{-1} \text{ s}^{-1}$ respectively. Individual left or right quantum dots could be formed separately within the 2DEG by energizing different sets of gates or alternatively a system of two few-electron dots in series could be achieved. Plunger gates 1B and 3B were used to tune the electrochemical potentials of the dots, and thereby the number of electrons confined in the dots. The techniques employed for emptying the dots and identifying the number of electrons have been described elsewhere.³ The conductance G was measured using standard low noise lock-in techniques with a typical bias voltage of $10 \mu\text{V}$.

We begin the experiment by forming the left and the right dots individually by energizing all the gates except pairs 3B-4B and 1B-0B, respectively. To characterize each dot we map out its addition spectrum in a perpendicular magnetic field. We focus on the regime near filling factor $\nu = 2$ in the dot for which the magnetic field induced ground state transitions (including spin transitions) are very well characterized from investigations of single quantum dot devices^{14,15,16} and the charge distribution scheme of single particle states is particularly simple. This regime includes both spin transitions and spatial charge redistribution events which can be used to probe the above ideas. In Fig. 1(b) we show a typical conductance greyscale of a single dot in the vicinity of the $\nu = 2$ transition. The magnetic field dependence of four CB peaks on the left dot is plotted. At $\nu = 2$ electrons occupy a simple ladder of states within the first Landau level (1LL) associated with an approximately parabolic confining potential in each dot.¹⁷ The wavefunction of each of these states can be regarded as a ring orbital with a radius that increases with the energy of the state. Each orbital state can be occupied by a pair of electrons with opposite spin. Reducing the magnetic field from its $\nu = 2$ value transfers an electron from the outermost orbital of the 1LL to the innermost orbital of 2LL. These transitions are reflected in the CB peak position^{14,16}. For a CB peak corresponding to the tunneling of a $N + 1$ electron through an N -electron dot ($N \leftrightarrow N + 1$ transition) both ground state transitions of the $N + 1$ and N electron dot are observed as cusps. When the $N + 1$ electron tunnels through the orbital of the 1LL (2LL) the magnetic field dependence of the position of the respective CB peak is characterized by a downward (upward) slope. An example of such behavior is shown in Fig. 1(c) for the $12 \leftrightarrow 13$ transition. The down (up) pointing arrow identifies the GS transition for a 13(12)-electron dot.

For an even number of electrons a spin flip is required during the transfer of an electron between the 1LL and 2LL and a singlet-triplet transition occurs for the $\nu = 2$ dot. These spin transitions are detected by means of spin blockade spectroscopy and result in a strong modulation of the CB peak amplitude, as seen in Fig. 1(b). One period of the observed amplitude modulation is shown in Fig. 1(c) for a $12 \leftrightarrow 13$ transition. When the spin-down electron tunnels through the edge orbital of the dot there is no blockade (NB) and a high conductance is observed. Tunneling of spin-up electrons through the same orbital occurs at a lower current since spin-up electrons are spin blocked (SB). Those two regimes are separated by a region of very low conductance due to a different blockade mechanism. The electron in this case tunnels through the innermost orbital, belonging to the 2LL. Since the coupling of this orbital to the leads is reduced due to the lateral geometry of the device we refer to this regime as being geometrically blocked (GB).

Two dots in series are formed by energizing all gates. Figure 2(a) shows the greyscale of conductance vs. plunger gates voltages. The plot, illustrating the peak

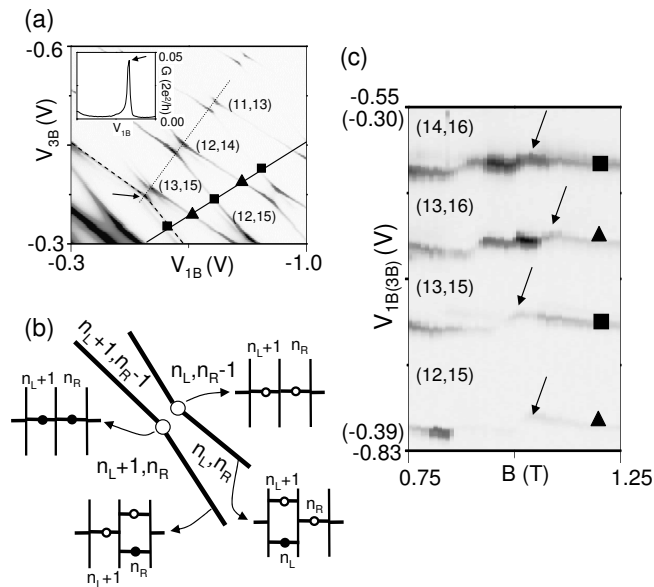


FIG. 2: (a) The measured charging diagram of the double dot. Inset shows how amplitude of CB peaks rapidly decreases away from the triple point (marked by an arrow); (b) schematic representation of different energy configurations of a double dot system close and away from triple points. Pair of numbers (n_L, n_R) describe occupation number for the left and right dot in each configuration. Open (closed) circles indicate empty (occupied) levels in the dot; (c) inverted conductance greyscale showing magnetic field dependence of four CB peaks, measured along the solid line marked in (a). Solid squares (triangles) mark peaks observed when only the left (right) dot is aligned with the leads. Arrows mark $\nu = 2$ transition as detected for each configuration.

positions in $(1B, 3B)$ plane, is the measured charging diagram of the double dot (DD) system, resembling the well-known “honeycomb” pattern.¹⁸ The configuration within each honeycomb is characterized by a pair of occupation numbers (n_L, n_R) , denoting the number of electrons in the left (n_L) and right (n_R) dot. Conductance is highest at the so-called triple points, at which the three neighboring configurations are degenerate. These points correspond to the situation when both dots are in-resonance with each other and with both leads, as is shown schematically in Fig. 2(b), so charge (current) can be easily transferred through the system. We investigated this regime in detail in Ref. 6 where we demonstrated the formation of molecular states near the $\nu = 2$ regime.

Let us now focus on the region away from the triple points. Along these sides of the honeycombs only two neighboring electron configurations are degenerate. This corresponds to the situation where only one of the dots is in resonance with the leads. As a result the conductance drops by over an order of magnitude, as shown in the inset in Fig. 2(a). A voltage scan along the solid line shown in Fig. 2(a) still results in a series of CB peaks but with each peak corresponding to a configuration with only one dot in resonance with the leads.

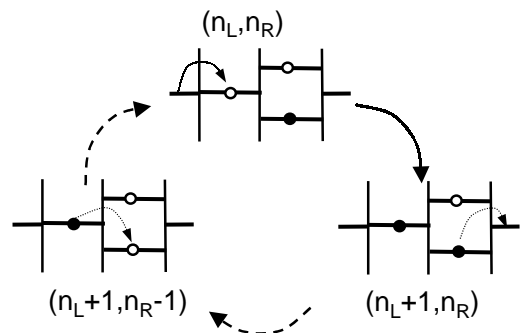


FIG. 3: Schematic representation of the configuration involved in the transfer of an electron through the double dot system when only the left dot is in resonance with the leads. Dashed arrows indicate co-tunneling events through the virtual $(n_L + 1, n_R - 1)$ configuration.

Fig. 2(c) reveals the magnetic field dependence of such a scan. Intuitively we would expect that the current amplitude through the system would reflect the properties of both dots (since states within both dots are involved in the current) but that the Coulomb blockade spectroscopy (i.e. peak position) would only probe the on-resonance dot (since the peak occurs when the electrochemical potential of this dot aligns with the leads). The picture emerging from the experiment suggests this is not the complete picture. We find three major features in the scan: (i) two adjacent peaks are not paired in their magnetic field behavior in contrast to peaks at the triple points;⁶ (ii) the observed amplitude modulation reflects transitions in ground states of both in-resonance and off-resonance dots as intuitively expected and interestingly (iii) the peak positions reflect the transitions occurring in both dots i.e. not only in the dot in resonance with the leads. The first of the above observations confirms that in the regime away from the triple points we are no longer dealing with molecular-like behavior in the double dot system, which now behaves as two dots in series. To analyze the second and third of the above findings we start with a discussion of tunneling through a DD system when only one dot is in resonance with the leads.

III. DISCUSSION

Let us consider the situation when the left dot is in resonance with the leads whereas the right dot is off-resonance. The initial configuration is characterized by a pair of occupation numbers (n_L, n_R) and is schematically represented in Fig. 3. The n_R level in the right dot lies below the Fermi energy of the leads and so it is occupied by an electron, while the n_L level in the left dot is empty. Since the n_L level is in equilibrium with the source lead an electron can tunnel back and forth between the source and the dot, i.e. the system configuration fluctuates between (n_L, n_R) and $(n_L + 1, n_R)$.

For the current to flow, however, the electron needs tunnel through the right dot. This is possible only if consider virtual transitions. The n_R electron leaves right dot to the lead, and a $(n_L, n_R - 1)$ configuration is reached. Simultaneously, in the co-tunneling process the $n_L + 1$ electron from the left dot enters the right dot, the configuration (n_L, n_R) is achieved again, however, an electron has been transferred through the device, i.e. current flows. We can write down the whole cycle as $(n_L, n_R) \rightarrow (n_L + 1, n_R) \rightarrow (n_L + 1, n_R - 1) \rightarrow (n_L, n_R)$ where $(n_L + 1, n_R - 1)$ is the virtual configuration reached through co-tunneling processes indicated in Fig. 1 by dotted lines. We now speculate that it is possible to decompose the cycle into the two relevant single dot transitions for the purpose of understanding the information obtained from the amplitude modulation. For the left dot the important transition is $n_L \rightarrow n_L + 1 \rightarrow n_L$ while for the right dot it is $n_R \rightarrow n_R - 1 \rightarrow n_R$. It is, of course, true that this is a virtual process and the number of electrons in the right dot is in reality fixed at n_R . However, if these transitions are suppressed (e.g. due to spin or spatial blockade) then the co-tunneling process will also be suppressed.

The above analysis is found to be consistent with experimental observations. As an example we check the top peak from the spectrum in Fig. 2(c), corresponding to the situation when $\mu_L(14)$ is aligned with the source lead and $\mu_R(16)$ is below the Fermi level of the leads. According to our previous discussion the transition $(13, 16) \leftrightarrow (14, 16)$ can be written down $(13, 16) \rightarrow (14, 16) \rightarrow (14, 15) \rightarrow (13, 16)$ and can be composed into $L13 \leftrightarrow 14$ and $R16 \leftrightarrow 15$ processes on the left and the right dot respectively. Let us therefore compare this peak with the single dot data related to transitions $L13 \leftrightarrow 14$ (left dot) and $R16 \leftrightarrow 15$ (right dot). The results are shown in Fig. 4. Fig. 4(a) shows inverted greyscale data of the relevant peaks from measurements obtained on the double dot system (middle panel) as well as single dot traces from the left dot (top panel) and the right dot (bottom panel). The single dot traces have been shifted by a small amount along horizontal axis, 40 mT (60 mT) for the left (right) dot trace, towards lower field values to match the positions of the unambiguous $\nu = 2$ transition. For reference the $(13, 15) \leftrightarrow (13, 16)$ peaks is also shown. The magnetic field values at which GS transitions occur in single dots are marked by arrows. For a $N \leftrightarrow N + 1$ transition an arrow pointing down (up) marks a ground state transition for a $N + 1(N)$ -electron dot. As described during the discussion of Fig. 1, these transitions result in step like features in the position of Coulomb blockade peaks with the cusps at the bottom (top) of the steps reflecting the $N(N+1)$ electron GS transitions. For reference we label all of these transitions with letters A...H, starting with the highest field transition, which over this range of magnetic fields is the transition into the $\nu = 2$ regime for the 16-electron dot ($R16 \leftrightarrow 15$ peak). For each peak these transitions divide the field range into several distinctive regions character-

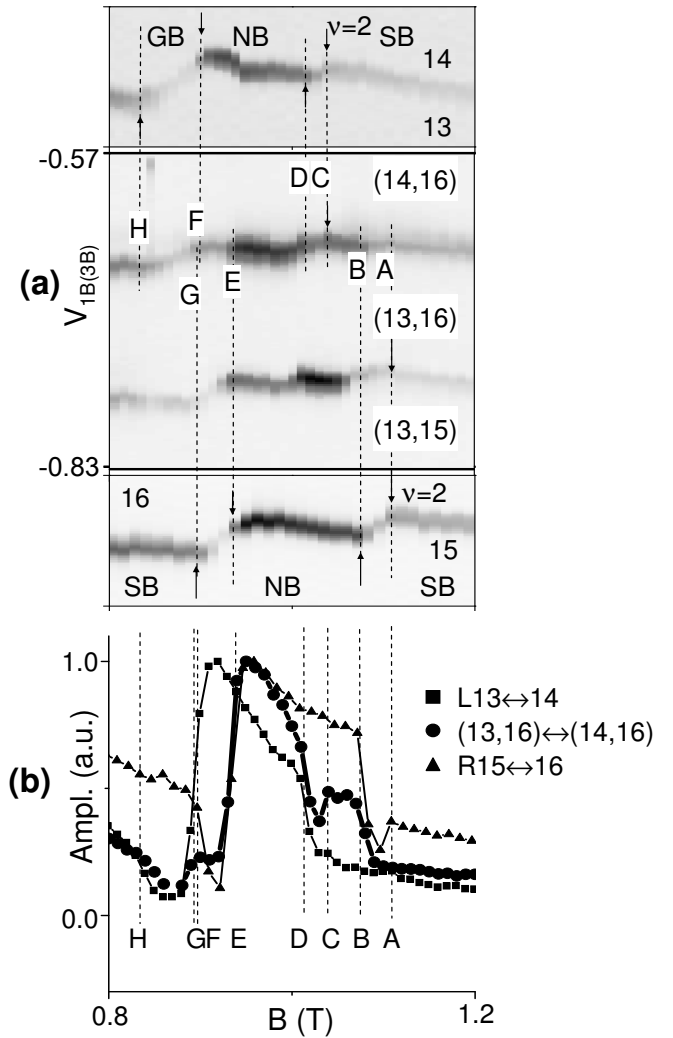


FIG. 4: Comparison of the double dot data for the $(13, 16) \leftrightarrow (14, 16)$ with single dot data for the $L13 \leftrightarrow 14$ and the $R15 \leftrightarrow 16$ transitions on the left and the right dot respectively in the vicinity of the $\nu = 2$ transition. (a) respective inverted greyscales of the double dot (middle panel), the left dot (top) and the right dot (bottom) data. As a reference shown is also a peak related to $(13, 15) \leftrightarrow (13, 16)$ transition; (b) extracted amplitude of respective CB peaks. Arrows and dashed lines mark transitions in ground states of respective dots, labeled by letters for the reference. For details see text.

ized by different amplitudes, which can be seen to reflect the amplitude modulation of the relevant single dot peaks over the same regime. The amplitude of the respective CB peaks are shown in the Fig. 4(b). The amplitude has been normalized to the highest value for each peak over the field range. It is clearly seen from the data that the conductance through the transition $(13, 16) \leftrightarrow (14, 16)$ is strongest in the region *DE* when *both* $L13 \leftrightarrow 14$ and $R16 \leftrightarrow 15$ transitions are the strongest on the individual dots i.e. when transport through the individual dots is non-blockaded. Whenever a GS transition in one of the dots causes a blockade mechanism to become ac-

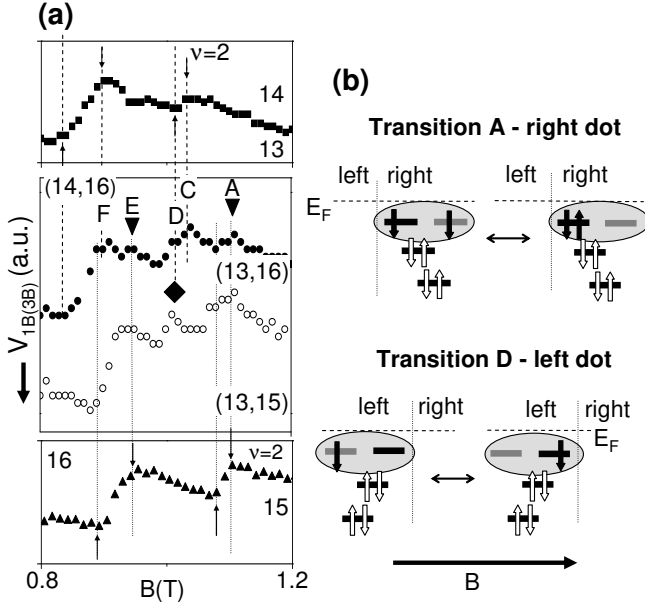


FIG. 5: (a) Peak positions of the data from Fig. 4(a). Curves were offset vertically for clarity. The thick arrow indicates the direction of higher negative plunger voltage. Ground state transitions on single dots are marked like in Fig. 4. Black triangles (diamond) mark features related to charge redistribution events occurring in the right (left) off-resonance dot and picked up by electrochemical potential of the in-resonance left (right) dot; (b) schematic representation of ground state transitions constituting charge redistributions. Horizontal dashed line marks the Fermi energy of the leads (E_F). Vertical dotted line marks the edge of both dots. Horizontal black (grey) bars indicate edge (center) orbitals of the 1LL (2LL). For details see text.

tive (either spin (SB) or geometrical (GB)) for either of the corresponding single dot transitions, the resulting co-tunneling current through the DD system decreases. Lowering the magnetic field below the E transition leads to decrease in current due to both GB and SB mechanisms for the off-resonance dot (region EF). For magnetic field values above the C transition, regions exist where only one of the two mechanisms is active. In the BC region the current is decreased due solely to the SB mechanism on the in-resonance dot, but is then further reduced when the SB mechanism is also switched on for the off-resonance dot after it undergoes a transition to the $\nu = 2$ regime (the A transition). Details of the amplitude pattern observed for all peaks from Fig. 2(c) provide a consistent picture. Firstly, we obtain direct information on which particular co-tunneling route is dominant. A quite different pattern, for example, would be expected if the co-tunneling was dominated by elastic co-tunneling through the unoccupied state in the off-resonance dot, i.e. through $\mu_R(17)$ in the above scenario. Secondly, a detailed analysis of the amplitude pattern¹⁵ confirms that spin blockade is active in limiting the co-tunneling current.

Let us now discuss the peak position in the double dot

traces. The peak positions of the identical data as in Fig. 4(a) are plotted in Fig. 5(a). Since the left dot is always aligned with the leads for the $(13, 16) \leftrightarrow (14, 16)$ peak, its position in $V_{1B,3B}$ reflects the spectroscopy of the addition spectrum of the left quantum dot associated with the transition $L(13) \leftrightarrow (14)$. Similarly for the $(13, 15) \leftrightarrow (13, 16)$ peak, the addition spectrum of the right dot associated with the $R(15) \leftrightarrow (16)$ transition is measured. It can be seen that the step-like behavior observed for single dot traces is reproduced in the double dot data. Upward/downward cusps observed in $L(13) \leftrightarrow (14)$ ($R(15) \leftrightarrow (16)$), reflecting GS transitions in 13/14 (15/16)-electron dots, align very well with the similar cusps on $(13, 16) \leftrightarrow (14, 16)$ ($(13, 15) \leftrightarrow (13, 16)$). It is important to note, however, that additional features are present in the peak positions of the double dot traces. A comparison with the single dot traces confirms that these are related to GS transitions in the off-resonance dot. The triangles mark the features observed in $(13, 16) \leftrightarrow (14, 16)$ peak as a result of GS transitions in the off-resonance right dot with $N = 16$ electrons. One of those transition (A) is shown schematically in the top panel of Fig. 5(b). As a result of this transition a spin up electron from the outermost occupied orbital of the 1LL (black horizontal bar) is transferred to the lowest orbital of the 2LL (grey horizontal bar), placed close to the center of the dot, as magnetic field is lowered. Due to the electrostatic coupling between the dots this redistribution of charge within the off-resonance dot causes a drop in the electrochemical potential of the in-resonance dot shifting the Coulomb blockade peak to more negative voltages as observed experimentally. Similar observations are seen for other transitions e.g. at the $(13, 15) \leftrightarrow (13, 16)$ transition, the charge redistribution in the off-resonance left dot with $N = 13$ (transition D) is picked up by the in-resonance right dot and reflected in the spectrum (feature marked by a black diamond in Fig. 5(a)). A related observation was made recently by Ref. 7 in the Kondo regime. This non trivial observation suggests that integrated quantum charge detectors (dots in series or quantum point contacts) can be used not only to detect a decrease or increase in the number of electrons occupying the quantum dot but also to detect rearrangements of the existing charge within a dot. Measurements using such techniques to detect more complex spin phenomena are currently under way.

IV. SUMMARY

In summary, we have presented results of coulomb blockade experiments on a double dot system with only one dot in resonance with the leads. In this regime the current through the system is driven by co-tunneling events through the off-resonance dots. The co-tunneling current reflects both geometrical and spin blockade phenomena occurring within each as well as between the two dots. In addition we found that charge rearrangements

at a fixed electron number on one of the dots are reflected in changes of the chemical potential of the other dot.

Acknowledgments

We would like to acknowledge useful discussions with P. Hawrylak, M. Korkusinski, S. Studenikin and D. G.

Austing. A.S. would like to acknowledge assistance from CIAR (Canadian Institute for Advanced Research).

-
- * Present address: Experimentelle und Angewandte Physik, University of Regensburg, D-93040 Regensburg, Germany.
 - ¹ M. A. Kastner, Phys. Today **46**, 24 (1993).
 - ² D. Loss and D. P. DiVincenzo, Phys. Rev. A **57**, 120 (1998).
 - ³ M. Ciorga, A.S. Sachrajda, P. Hawrylak, C. Gould, P. Zawadzki, S. Jullian, Y. Feng, and Z. Wasilewski, Phys. Rev. B **61**, R16315 (2000).
 - ⁴ A. Sachrajda, P. Hawrylak and M. Ciorga, Nanospintronics with quantum dots, in *Electron Transport in Quantum Dots*, edited by J.P. Bird (Kluwer Academic Publishers, Dordrecht, 2003).
 - ⁵ J. M. Elzerman, R. Hanson, J. S. Greidanus, L. H. Willems van Beveren, S. De Franceschi, L. M. K. Vandersypen, S. Tarucha, and L. P. Kouwenhoven, Phys. Rev. B **67**, 161308 (2003).
 - ⁶ M. Pioro-Ladriere, M. Ciorga, J. Lapointe, P. Zawadzki, M. Korkusinski, P. Hawrylak, and A. S. Sachrajda, Phys. Rev. Lett. **91**, 26803 (2003).
 - ⁷ D. Sprinzak, Y. Ji., M. Heiblum, D. Mahalu, and H. Shtrikman, Phys. Rev. Lett. **88**, 176805 (2002).
 - ⁸ L. P. Kouwenhoven, C. M. Marcus, P. McEuen, S. Tarucha, R. Westervelt and N. S. Wingreen, Electron Transport in Quantum Dots in *Mesoscopic Electron Transport*, edited by L. L. Sohn, L. P. Kouwenhoven and G. Schon, NATO ASI Series E 345 (Kluwer, Dordrecht, 1997).
 - ⁹ A.S. Sachrajda, P. Hawrylak, M. Ciorga, C. Gould, P. Zawadzki, Physica E **10**, 493 (2000).
 - ¹⁰ D. V. Averin and Yu. V. Nazarov, Macroscopic Quantum Tunneling of Charge and Co-Tunneling, in *Single Charge Tunneling*, edited by H. Grabert and M. H. Devoret, NATO ASI Series (Plenum Press, New York, 1992).
 - ¹¹ S. M. Cronenwett, S. R. Patel, C. M. Marcus, K. Campman, and A. C. Gossard Phys. Rev. Lett. **79**, 2312 (1997).
 - ¹² S. De Franceschi, S. Sasaki, J. M. Elzerman, W. G. van der Wiel, S. Tarucha, and L. P. Kouwenhoven Phys. Rev. Lett. **86**, 878 (2001).
 - ¹³ D. Goldhaber-Gordon, H. Shtrikman, D. Mahalu, D. Abusch-Magder, U. Meirav, M. A. Kastner, Nature **391**, 156 (1998).
 - ¹⁴ M. Ciorga, A.S. Sachrajda, P. Hawrylak, C. Gould, P. Zawadzki, Y. Feng, and Z. Wasilewski, Physica E **11**, 35 (2001).
 - ¹⁵ M. Ciorga, A. Wensauer, M. Pioro-Ladriere, M. Korkusinski, J. Kyriakidis, A. S. Sachrajda, and P. Hawrylak, Phys. Rev. Lett. **88**, 256804 (2002).
 - ¹⁶ S. Tarucha, D.G. Austing, Y. Tokura, W.G. van der Wiel, and L.P. Kouwenhoven, Phys. Rev. Lett. **84**, 2485 (2000).
 - ¹⁷ A. Wensauer, M. Korkusinski and P. Hawrylak, Phys. Rev. B **67**, 35325 (2003).
 - ¹⁸ W.G. van der Wiel, S. De Franceschi, J. M. Elzerman, T. Fujisawa, S. Tarucha, and L. P. Kouwenhoven, Rev. Mod. Phys. **75**, 1 (2003).